

# HEAD AND SPINAL TRAJECTORIES IN CHILDREN AND ADULTS EXPOSED TO LOW SPEED FRONTAL ACCELERATION

**Sriram Balasubramanian, PhD**

**Thomas Seacrist, MS**

**Matthew R. Maltese, MS**

**Kristy B. Arbogast, PhD**

Center for Injury Research and Prevention

The Children's Hospital of Philadelphia

USA

**Terrance Hopely, BS**

**Eric Constans, PhD**

Department of Mechanical Engineering

Rowan University

USA

**Robert Sterner, PhD**

Department of Health and Exercise Science

Rowan University

USA

**Hiromasa Tanji**

**Kazuo Higuchi**

Takata Corporation

Japan

Paper Number 09-0263

## ABSTRACT

Head injuries are the most common injuries sustained by children in motor vehicle crashes. Prevention of these injuries through advances in vehicles and restraint systems requires a biofidelic anthropomorphic test device (ATD). Pediatric ATDs are primarily developed from scaling down adult volunteer and cadaver impact test data. Limited experimental data exist on pediatric head and neck kinematics in order to evaluate the biofidelity of the ATDs. The aim of the current study was to evaluate the head and spinal kinematics of pediatric and adult volunteers in response to a dynamic low-speed frontal sled test. Low speed volunteer testing of five male subjects in each of two specific age groups (9-12, and 18-30 years) were performed using a pneumatically actuated – hydraulically controlled sled. Safe limits were established from measurement of bumper car accelerations at an amusement park ride (4.9 g, 55.7 msec rise time, 110 msec duration), which we believed to be sub-injurious to the adult and child amusement park population. We subsequently recreated the bumper car environment in the laboratory, by developing a low-speed hydro-pneumatic sled. As an added measure of safety, our average maximum cart acceleration was 3.59 g for children and 3.78 g for adults, thus producing occupant loads that are approximately 25% less than the bumper car amusement park ride. Spherical reflective markers were placed on the head, neck,

torso, upper and lower extremities and tracked using a 3D motion analysis system. An angular rate sensor was mounted to a bite plate of an athletic mouth guard to measure the head rotational velocity. Electromyography sensors were attached to key muscle groups to measure the muscle response of the subjects to the loading environment. Each subject was subjected to six sled runs. Head and neck trajectories were compared between the adult and pediatric subjects. In addition, the effect of habituation on kinematic response was examined by comparing within subject changes in kinematics throughout the series of six sled runs.

## INTRODUCTION

Traumatic brain and skull injuries are the most common serious injuries sustained by children in motor vehicle crashes regardless of age group, crash direction, or restraint type (Arbogast et al. 2005; Arbogast et al. 2002; Durbin et al. 2003; Howard et al. 2003; Orzechowski et al. 2003; Arbogast et al. 2004). Head injuries are responsible for one-third of all pediatric injury deaths (Adekoya et al. 2002; Thompson and Irby 2003) and are particularly relevant clinically as the developing brain is difficult to evaluate and treat. Prevention of these injuries through effective motor vehicle safety systems requires a biofidelic anthropomorphic test device (ATD) to ensure safety systems mitigate injuries in real children. The extent to which the pediatric ATD

accurately predicts the dynamics and kinematics of the occupant's head and spine in particular restraint and crash conditions directly influences safety system design and thus injury potential.

A growing body of evidence points to critical differences in spinal kinematics between humans and ATDs in the same restraint system. Compliance in the thoracic and cervical spine is a primary cause of this difference. The human spine is a relatively mobile, multi-segmented system, while the Hybrid III dummy's thoracic spine is essentially rigid. This difference in spinal compliance can generate differences in the head trajectory of the dummy relative to a human. Studies have shown that crash environments that would be defined as non-injurious based on a dummy's response can actually generate substantial injuries to the head, neck, and thorax of a cadaver since increased compliance in the spine creates an entirely different head trajectory and results in severe head contact with interior vehicle structures. (Shaw et al. 2001)

The same phenomenon has been demonstrated in the pediatric literature where the thoracic spine of the pediatric ATD has been shown to be much stiffer than that of a real child (Sherwood et al. 2003). This sled-based data compared pediatric post mortem human subjects (PMHS) data from the 1970s (Kallieris et al. 1978) with Hybrid III 6 year old ATD response and demonstrated the inaccurate predictions of a child's head trajectory and total forward excursion as well as the development of unrealistically high moments at the OC-C1 junction. As pediatric PMHS data is extremely limited, additional evidence on kinematic differences between pediatric ATDs and live humans comes from comparison of laboratory findings to field accident data. In many sled and vehicle frontal crash tests using pediatric ATDs, the published thresholds for the cervical spine injury metrics, Nij and neck tension, as well as the Head Injury Criterion (HIC) are often exceeded (Menon et al. 2003; Sherwood et al. 2003; Malott et al. 2004). Experience in incorporating pediatric ATD's in the rear seat of NHTSA's frontal NCAP tests and in development of enhancements to FMVSS 213 resulted in the ATD's inability to meet the proposed head and neck tolerance criteria. (Kuppa 2005) These results are at odds with several reports on the rarity of cervical spine injuries in child restraints and booster seats in the field and the overall effective protection of these restraints (Durbin 2002; Arbogast et al. 2002; Zuckerman et al. 2004).

These biofidelic inaccuracies are due in part to the pediatric ATD's spinal construction as a single steel beam rather than the multi-segmented, multi-degree-of-freedom complex structure characteristic of real children. As a result, the actual injury risk to a human child exposed to a similar collision environment may be overstated potentially providing misdirected guidance for restraint design. To further confound the issue, the effects of the non-biofidelic spine of the ATD's are restraint system dependent (Shaw et al. 2001). Thus, comparisons of alternative design concepts may be skewed due to poor predictions of head trajectory and thus inaccurate assessment of head injury risk.

Traditionally, improvements in ATD biofidelity are achieved through rigorous evaluation of PMHS impact testing. Although this approach is an accepted method for obtaining adult ATD design specifications, child PMHS data is limited and thus current pediatric ATD's are based on adult biomechanical test data scaled to account for geometric and material differences between adults and children, to the extent such data is available. However, during the human developmental process, local and regional anatomical structures change in ways that are not quantitatively considered in the scaling processes. Thus, to address this limitation and improve the ability of the current pediatric ATDs to mimic the interaction of real children with a restraint system, novel methods for determining pediatric dynamic response are required.

Human volunteer experiments have a long established history in biomechanics research. Early researchers used themselves as test specimens (Stapp 1949) or enrolled adult human volunteers to define the dynamic response of the head and neck to trauma (Ewing et al. 1968; Mertz and Patrick 1971; Wismans et al. 1987). To our knowledge, no data exists on the dynamic response of the head and neck of children relative to the automotive environment. Therefore the objective of this research was to develop a methodology to safely study the sub-injurious kinematics of child volunteers in dynamic automotive-like events and through testing of adult volunteers in a similar loading environment, evaluate the effect of age on the kinematic response. This paper describes the methodologic development of the test protocol and provides exemplary data from both the child and adult test subjects.

## **METHODS**

This study protocol was reviewed and approved by the Institutional Review Boards at The Children's

Hospital of Philadelphia, Philadelphia, PA and Rowan University, Glassboro, NJ.

### Test device

A pneumatically actuated – hydraulically controlled ‘low-speed acceleration seating buck’ (LASB) shown in Figure 1, was designed to subject restrained human volunteers to a sub-injurious, low-speed frontal crash pulse.

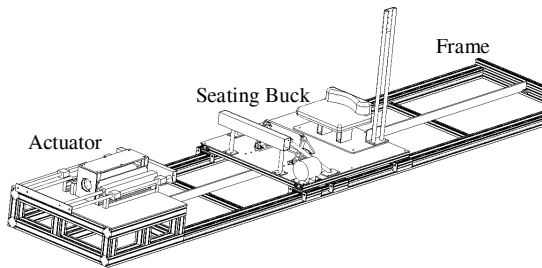


**Figure 1. Schematic of the low-speed acceleration seating buck (LASB).**

The LASB is primarily comprised of three sub-assemblies, namely frame, actuator and seating buck. The frame for the LASB was constructed of extruded aluminum tubing (MiniTec Framing Systems LLC, Victor, NY). The structural framework included a platform (for the actuator assembly) which was rigidly connected to two 18 feet long parallel support rails with equally spaced cross members for rigidity. A steel bar between the two support rails served to slow the sled to a stop following the primary acceleration pulse. The actuator assembly was comprised of a pneumatic actuator (Mc Master-Carr, Robbinsville, NJ) (diameter – 4 inches, stroke length – 20 inches, operating pressure – 200 psi) connected to an opposing dual hydraulic piston-cylinder (Model TZ22, Vickers Cylinders, Eaton Corporation, Cleveland, OH) arrangement using a rigid frame. A 2-way high dynamics proportional throttle cartridge valve (Model LIQZO-LE, Atos, Italy) was used in the custom-designed hydraulic circuit to control the displacement profile of the pneumatic actuator. When the pneumatic actuator was fired, it delivered the impact force to the seating buck.

The seating buck assembly (Figure 2) framework was also constructed using extruded aluminum tubing (MiniTec Framing Systems LLC, Victor, NY). It was comprised of a moving platform mounted on the two support rails by means of six low friction linear bearings. A custom-built impact fixture was mounted on the platform to transfer the force from the pneumatic actuator to the moving platform. A rigid low-back padded seat, an adjustable height

shoulder belt anchor post (similar to a B-pillar in an automobile), lap belt anchors and an adjustable footrest were mounted on the platform. The low-back seat allowed for the motion analysis markers along the spine to be visible to the cameras. A standard automotive three-point belt system was attached to the lap belt and shoulder belt anchor points. An onboard pneumatic braking system was provided to interact with the braking rail to decelerate the moving platform. In order to limit the excursion of the subject during rebound associated with braking, a nylon strap was attached to two vertical bars behind the seat (at the location of T4).

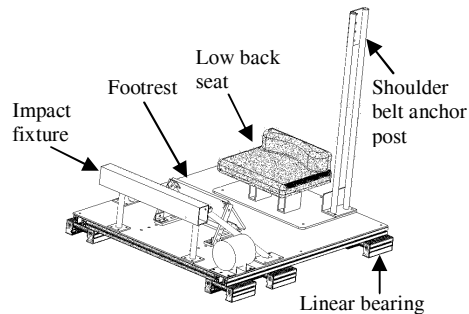


**Figure 2. Schematic of the seating buck assembly.**

### Safe volunteer crash pulse

An amusement park bumper car ride was studied to provide a benchmark of a crash-like situation commonly and safely used by children for recreation and enjoyment. Safe limits on the volunteer crash pulse were defined from measuring a bumper car-to-wall impact in an amusement park (Six Flags Great Adventure, Jackson, NJ). An accelerometer was secured to the rigid cross-member of the steering assembly of a bumper car. The car was used in its typical usage patterns, impacting the wall of the arena, another vehicle head to head, and another vehicle in a T-type configuration. This process was repeated with two different bumper car vehicles. The maximum pulse obtained was 4.9 g in 55.7 msec (Figure 3). This was defined as the envelope of safety for the human volunteers.

### Design considerations for safety

Additional safety evaluations were performed during the design and operation of the LASB to ensure safety, comfort and protection of the human subjects. Firstly, the restraints of the amusement park bumper car were studied and the LASB restraints were designed to provide more custom-fit protection. The amusement park bumper cars provided restraint through two load paths – 1) a loop of belt across the torso, and 2) a footrest that restrained the lower extremities. The bumper car restraints were not

adjustable for different size occupants. The LASB, in contrast, features a customizable restraint system to distribute test forces over three load paths: 1) torso loads are carried by a shoulder belt that rests on the clavicle, 2) pelvic loads by a lap belt, and 3) lower extremity loads by the foot rest. The LASB belt and foot rest are fully adjustable to maximize occupant comfort, ensuring that that shoulder belt passes over the clavicle and sternum, that the lap belt engages the iliac wings, and that the leg restraints are adjustable to allow a bent knee. Thus, because the LASB restraints distribute forces through more load paths than the traditional bumper car restraint, and provide adjustability for optimal fit, we expect that the pressure applied by the restraints to the test subjects to be lower in magnitude and more optimally placed than a typical bumper car.

As further confirmation of the safety of this event, a literature review on sub-injurious loading to human volunteers was performed. All of this literature uses adult human subjects, as there is no data on children, however we believe the findings are relevant to our study and support the safety of our test environment. First in the amusement environment, the top 7 roller coaster rides by *g*-loading in the United States in 2001 exposed occupants to accelerations of 5 to 6.5 *g* (Braksiek and Roberts, 2002). Roller coaster loading likely differs in loading direction, duration and onset rate and thus limit our ability to directly compare roller coaster data to the volunteer sled. More direct comparisons can be obtained from Ewing et al. (1968) who measured the dynamic response of the head and neck by exposing seated and restrained adult human volunteers to a frontal peak sled acceleration of 2.8 *g*. Mertz and Patrick (1971) subjected a human volunteer to frontal sled plateau accelerations ranging from 2 to 9.6 *g*. Although low levels of acceleration (<8 *g*) were well tolerated by the volunteer, he experienced neck pain beyond 8 *g*. This review further confirms that the acceleration levels at which the LASB is designed have previously been tolerated safely by human volunteers.

Lastly, the design of the LASB itself had several safety mechanisms through which the application of the low-speed acceleration was controlled. The hydraulically controlled – pneumatic powered actuator system was designed to deliver an acceleration pulse with a maximum acceleration of less than 4.5 *g* with a rise time of 50-70 msec – within the defined safety envelope. However, the subjects received a slightly lower pulse (shown in the results section). Other safety system redundancies included:

1. Well documented countdown procedure, safety check list and testing protocol
2. Manual pressure checks at the pneumatic and hydraulic accumulators equipped with pressure relief valves
3. Synchronized trigger circuit with key operated ‘arm’ switch and push button ‘fire’ switch to operate all systems simultaneously
4. Warning light on control box when system is ‘armed’ and ready to be fired
5. On board pneumatic system activated braking calipers on the front and back of the moving platform
6. Emergency braking system consisting of two hydraulic dampers mounted at the end of the rails
7. Multiple abort switches for each system
8. Fail safe volunteer-controlled abort contact-switch

These safety checks ensured that the LASB delivered the appropriate pulse and could only be triggered and actuated when the test area of the LASB was cleared by personnel and the subject was appropriately restrained and ready for testing. Dynamic proof testing of the LASB and all components was also completed prior to human volunteer testing.

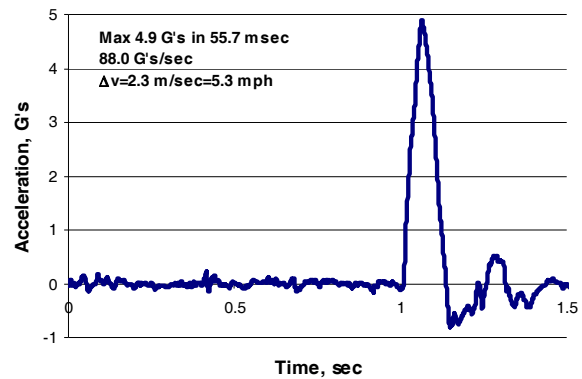


Figure 3. Bumper car to wall acceleration pulse.

### Human Subjects

**Inclusion criteria** – Specific inclusion criteria were male subjects aged between 6 and 40 years whose height, weight and BMI were within 5<sup>th</sup> and 95<sup>th</sup> percentile for the subject’s age (based upon CDC growth charts for children (CDC Growth Charts, 2000) and CDC NHANES data for subjects 18+ years (NHANES data, 1994)). Subjects with existing neurologic, orthopedic, genetic, or neuromuscular conditions, any previous injury or abnormal pathology relating to the head, neck or spine were excluded from the study. Subjects were recruited

from flyers placed in the community and throughout CHOP and Rowan sites. Prior to the testing dates, telephone interviews were conducted with the adult subjects and parent / guardian of child subjects to confirm eligibility.

For the analyses presented herein, a total of 10 male subjects – five subjects in each of the two age groups (9-12 years and 18-30 years) were tested. Upon arrival at the test site, the study was explained in detail to all subjects including a demonstration of how the LASB functions by firing the sled without an occupant. The adult subjects were given a self-consent letter and the parent / guardian of the child subjects were given a parental consent letter with a child subject assent. After the subjects had been consented, height and weight were measured to verify that their height, weight and body mass index (BMI) were consistent with the inclusion criteria.

The subjects were asked to remove their shirt(s) to facilitate placement of the instrumentation and the following anthropometric measurements:

1. Head medial-lateral width at the level of nasion
2. Head anterior-posterior depth at the level of opisthocranium
3. Head girth at the level of opisthocranium
4. Head length from head top to mandible
5. Neck medial-lateral width at the level of C3-C4
6. Neck anterior-posterior depth at the level of C3-C4
7. Neck length (Opisthocranium to C7)
8. Neck girth at the level of C3-C4
9. Chest medial-lateral width at Xyphoid process
10. Chest anterior-posterior depth at Xyphoid process
11. Shoulder width (distance between left and right acromion processes)
12. Distance between Suprasternal notch to Xyphoid process
13. Seated height measured from head top to seat top
14. Waist girth at umbilicus
15. Hip width at Iliac crests
16. Buttock to Popliteal length
17. Knee to foot distance measured from lateral femoral condyle to floor

### **Instrumentation**

**Subject** – Spherical reflective markers (10 mm diameter) were placed on the head, neck, torso, upper and lower extremities and tracked using a 3D motion analysis system (Model Eagle 4, Motion Analysis Corporation, Santa Rosa, CA). Specifically, the photoreflective targets were attached to the following anatomical landmarks:

1. Head – On a tight-fitting elastic cap (Left and right temple, top and front of head in two places along the mid-sagittal plane, and on the occiput posteriorly), nasion and anterior to the left and right external auditory meatus.
2. Spine – Spinous processes of C4, T1, T4, T8, and L1.
3. Upper Extremity – Lateral humeral epicondyle, and ulnar styloid, all bilaterally
4. Torso – Acromion process (bilaterally), suprasternal notch, and Xiphoid process
5. Pelvis and Lower Extremity – Anterior superior iliac spine, lateral femoral epicondyle, lateral malleolus all bilaterally.

A comprehensive list of all the markers is provided in the Appendix – Table A1. An angular rate sensor – ARS (Model ARS-300, DTS Inc, Seal Beach, CA) was mounted via a custom fixture to a subject-specific athletic mouth guard to measure the head rotational velocity. Surface Electromyography (EMG) sensors were attached bilaterally to key muscle groups of the neck (Sternocleidomastoid, Paraspinous and Trapezius), lower torso (Erector Spinae), and lower extremities (Rectus femoris) to measure the muscle response of the subjects to the loading environment. A grounding electrode was centered over the right mastoidale. A telemetric Surface EMG system, Noraxon – TeleMyo 2400T V2 (Noraxon USA Inc, Scottsdale, AZ) was used to record the EMG signals. For each subject, their maximum isometric contraction for these muscles was measured prior to sled testing.

**LASB** – Spherical reflective markers were also placed on various locations on the seating buck and tracked using a 3D motion analysis system (Model Eagle 4, Motion Analysis Corporation, Santa Rosa, CA). A piezoresistive accelerometer (Model 7264-200, Endevco, San Juan, CA) was mounted to the moving platform frame to record the acceleration of the LASB. Lightweight belt webbing load cells (Model 6200FL-41-30, Denton ATD Inc, Rochester Hills, MI) were attached five inches from the D-ring location on the shoulder belt and on the inboard and outboard locations on the lap belt, respectively. Six-axis load cells was placed under the seat pan (Model IF-217, FTSS, Plymouth, MI) and footrest (Model IF-234, FTSS, Plymouth, MI), respectively to measure the reaction forces exerted by the subjects. A high-speed video camera (MotionXtra HGTH, Redlake, San Diego, CA) was placed sagittally to record the event at a rate of 1,000 frames per second (fps). In addition, two standard video camcorders (Model DC20, Canon Inc., Japan) were used to capture the frontal and sagittal views at 30 fps. The

hydraulic controller, Motion Analysis, T-DAS, EMG and high speed camera systems were triggered synchronously using a custom made circuit.

**Testing**

After the instrumentation setup was completed, the subjects were seated in the LASB as shown in Figure 4. The torso and knee angles were maintained at 110 degrees by adjusting the position of the footrest and nylon strap to mimic the posture of a seated occupant in an automobile (Reed et al. 2005). The shoulder belt angle at the D-Ring (defined as the angle the shoulder belt makes with the horizontal) and lap belt buckle angle (defined as the angle the lap belt buckle makes with the horizontal) were set at 70 degrees at initial position for all the subjects. In order to minimize the effect of initial head position, the subjects were asked to focus at a point placed directly in front of them at the level of their nasion. The lap and shoulder belts were then adjusted and secured to fit optimally for the subject’s size.

The experimental procedure with the LASB is a series of six tests, with each successive test designed to encourage the occupant to relax their muscles and allow the restraints to support their weight during the acceleration event, thus simulating the condition of an unbraced occupant in a frontal vehicle crash whose inertial forces are supported by the restraint system in the vehicle. Subjects received a countdown in each test prior to firing of the actuator. Each subject was given the option to either continue or withdraw from further testing at the completion of each test run. All the tests were conducted identically with a rest period of approximately 10 minutes between subsequent tests.

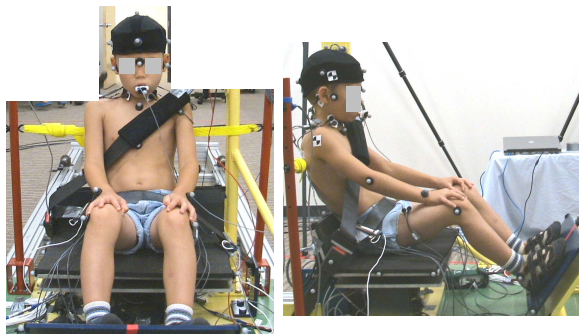


**Figure 4: Child subject seated in LASB.**

**Data acquisition and analyses**

Signals from the ARS, accelerometer and load cells were sampled at 10,000 Hz using a T-DAS data acquisition system (Diversified Technical Systems Inc., Seal Beach, CA) with a built-in anti-aliasing

filter (4,300 Hz). The Motion Analysis data were acquired at 100 Hz and analyzed using EVaRT5 software (Motion Analysis Corporation, Santa Rosa, CA). MyoResearch XP software was used to export the EMG data into ASCII format. The T-DAS, Motion Analysis and EMG data processing were automated using MATLAB 8.0 (The Mathworks Inc, Natick, MA). The high-speed video data were analyzed with Falcon software (Falkner Consulting for Measuring Technology GmbH, Gräfelfing-Lochham, Germany).

For the analyses presented herein, only the Motion Analysis data and the sled acceleration data will be discussed. The sled acceleration data were filtered at SAE channel frequency class (CFC) 60, as recommended by the SAE J211 standards.

**RESULTS**

The age, height, weight and BMI for the subjects whose data are presented herein are listed in Table 1.

**Table 1. Height, Weight and BMI for subjects**

Subject #	Age years	Height cm	Height Percentile	Weight kg	Weight Percentile	BMI kg/m <sup>2</sup>	BMI Percentile
11	9	124	5	25.1	17	16.3	51
8	10	136	31	28.5	22	15.4	23
18	10	144	68	33.1	47	16	32
16	12	165	92	50.3	74	18.5	54
19	12	155	68	40.3	41	16.8	29
21	22	172	38	64.8	14	21.7	31
23	22	176	51	86.6	65	28	66
24	22	180	69	106.6	94	32.8	93
22	24	169	22	73.4	37	25.8	47
27	30	180	69	80.7	53	24.8	39

For Child subjects, ages 6-18 years: Height, Weight and BMI percentiles were calculated using the CDC growth charts (2000)

For Adult subjects, ages 20+ years: Height, Weight and BMI percentiles were calculated using the NHANES data (1994)

The individual and averaged sled acceleration pulse for a set of six trials on a single subject is shown on Figure 5. The activation of the synchronous trigger (henceforth called ‘time zero’) was followed by a time delay before the movement of the sled (event). The time delay (approximately 100 msec) was attributed to the response lag associated with the LASB hydraulic system. Event onset (vertical line in Figure 5) was defined as the time at which the sled acceleration reached 5% of its peak value.

The five phases of the event are outlined below:

1. Acceleration – This is the first phase of the event that immediately follows event onset and corresponds to the pre-programmed acceleration pulse of the sled.

2. Restraint loading – The subject loads the seatbelt restraints.
3. Rebound – After maximum excursion, the subject rebounds back and interacts with the nylon strap behind the seat.
4. Coasting – During this phase, the sled coasts on the rails.
5. Braking – The pneumatic brakes are applied during this phase causing the gradual deceleration of the sled.

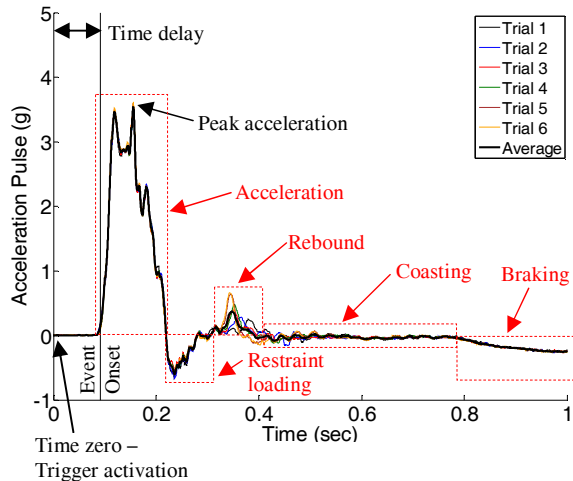


**Figure 5. Sled acceleration pulse of six individual trials and their average for a single human volunteer. Various phases of the event are shown in red – dashed boxes.**

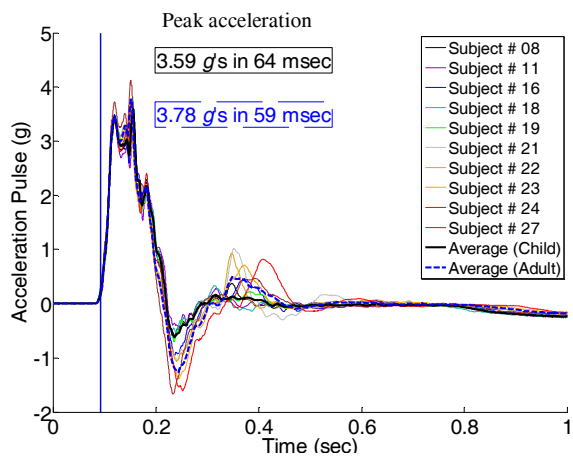


**Figure 6. Average sled acceleration pulse with peak values for child and adult subjects.**

The sled acceleration pulse from the six trials for each subject were averaged and plotted for the two age groups – child and adult (Figure 6). The children had slightly lower average peak acceleration (3.59 g)

with slightly longer rise time (64 msec) compared to adults (3.78 g in 59 msec).

The marker on the right rear of the cart (‘Cart back right – CBR #32’) was chosen as the reference point (origin) for the local coordinate axes shown in Figures A1a and A1b (Appendix). All marker trajectories were plotted with respect to this reference point. As an example, the head top marker trajectories were plotted along the sagittal plane (X-Z plane) for each of the six trials and averaged in time. An exemplar head top trajectory for a child and adult subject is shown in Figures 7a and 7b, respectively. Standard deviation bars in X and Z, indicating the variability among the six trials, were plotted at 100 msec intervals for a total duration of 600 msec.

The start point for each trajectory coincides with time zero. The average head top trajectories for the child and adult groups are shown in Figures 8a and 8b, respectively. The variation in the initial position of the trajectory start point between subjects can be attributed to the difference in seated height (Z-axis) and initial fore-aft head position (X-axis). The range of total displacement for the head top marker in the pediatric population was 298 – 371 mm (X-axis) and 38 – 109 mm (Z-axis). Similarly, the total displacement ranges for head top marker in the adult population were 297 – 463 mm (X-axis) and 35 – 79 mm (Z-axis).

The average trajectories for the C4 marker are shown on Figures 9a and 9b. The range of total displacement for the C4 marker in the pediatric population was 180 – 260 mm (X-axis) and 41 – 90 mm (Z-axis). Similarly, the total displacement ranges for C4 marker in the adult population were 211 – 294 mm (X-axis) and 40 – 77 mm (Z-axis). The average left iliac crest (pelvis) marker trajectories are shown on Figures 10a and 10b. The range of total displacement for the pelvis marker in the pediatric population was 81 – 128 mm (X-axis) and 15 – 36 mm (Z-axis). Similarly, the total displacement ranges for pelvis marker in the adult population were 138 – 167 mm (X-axis) and 18 – 38 mm (Z-axis).

The average trajectories for the left and right acromion markers were plotted in the transverse plane (X-Y plane) along with the schematic of a subject in the initial position (Figures 11a and 11b). Both the left and right marker trajectories remained almost perpendicular to this plane throughout the test. This is indicative of a lack of rotation of subjects about their Z-axis during the acceleration, restraint loading and rebound phases.

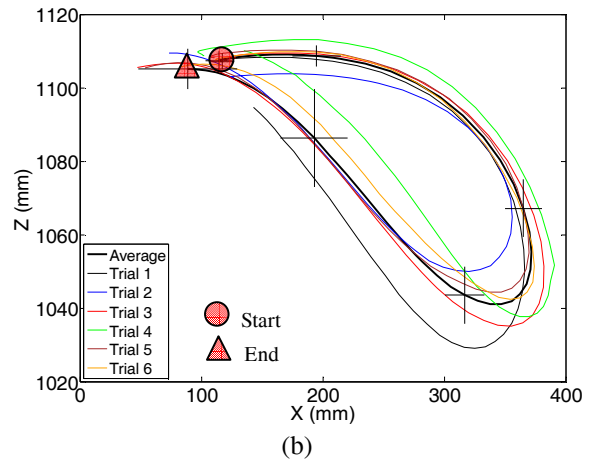
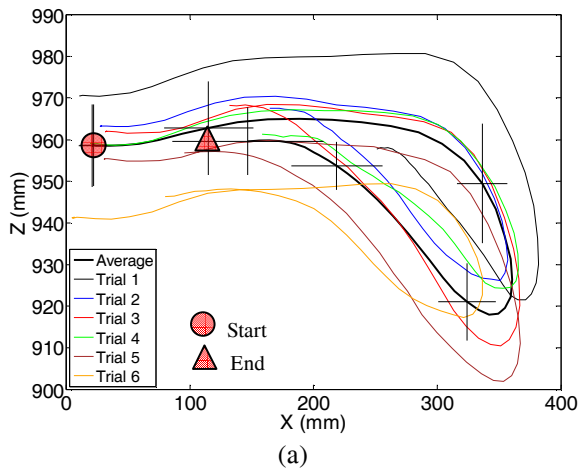


**Figure 7. Individual and average (with standard deviation bars in X and Z) head top marker trajectories in the sagittal plane for an exemplar (a) child and (b) adult subject.**

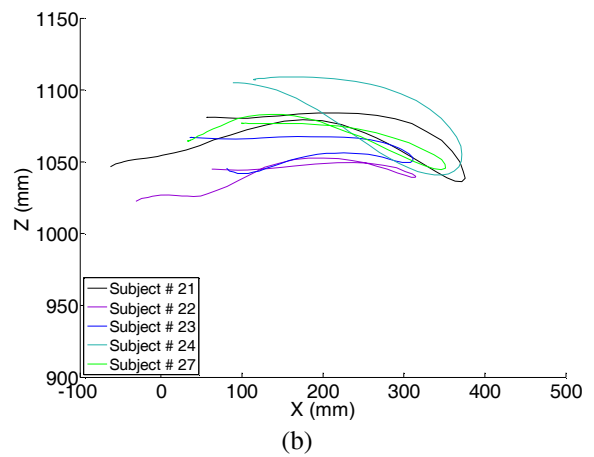
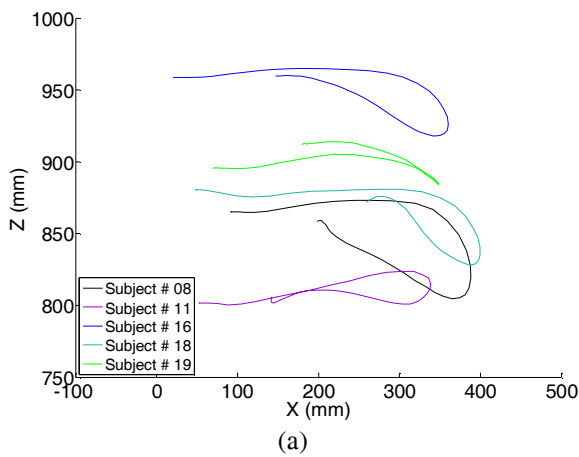


**Figure 8. Subject-Average head top marker trajectories in the sagittal plane for the (a) child and (b) adult group.**

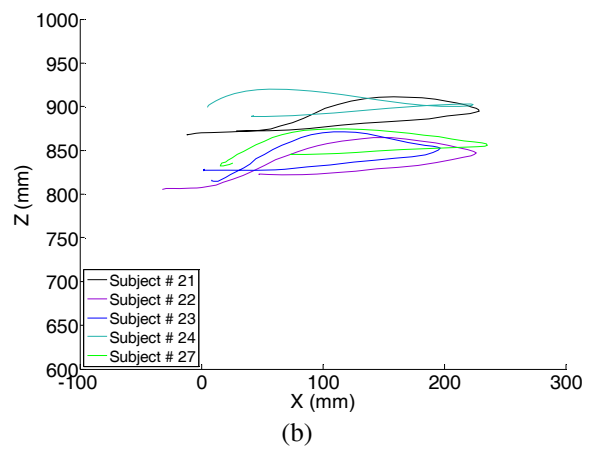
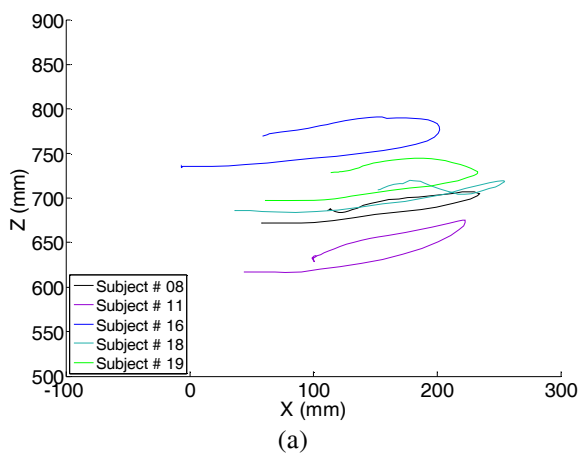


**Figure 9. Subject-Average C4 marker trajectories in the sagittal plane for the (a) child and (b) adult group.**

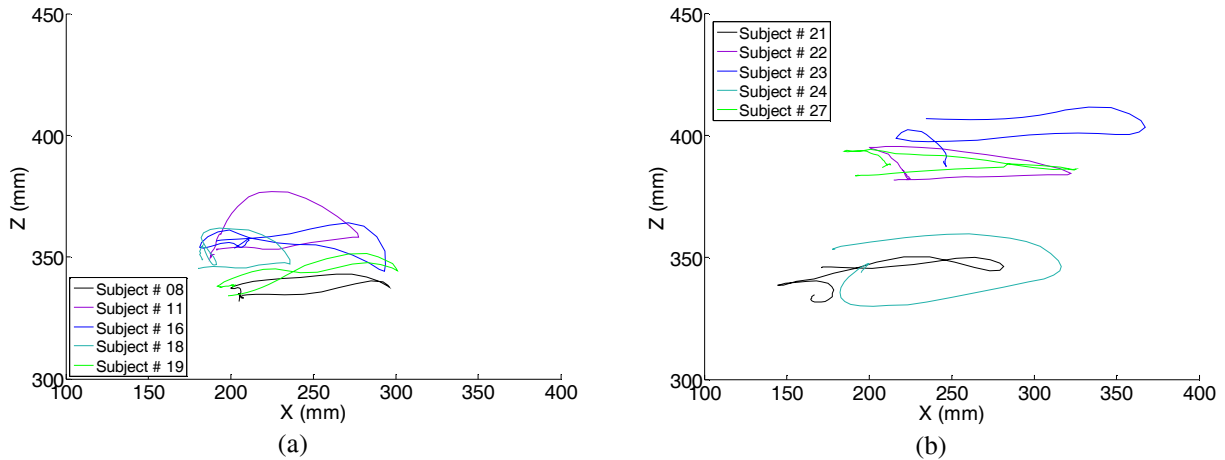


**Figure 10. Subject-Average left iliac crest marker trajectories in the sagittal plane for the (a) child and (b) adult group.**

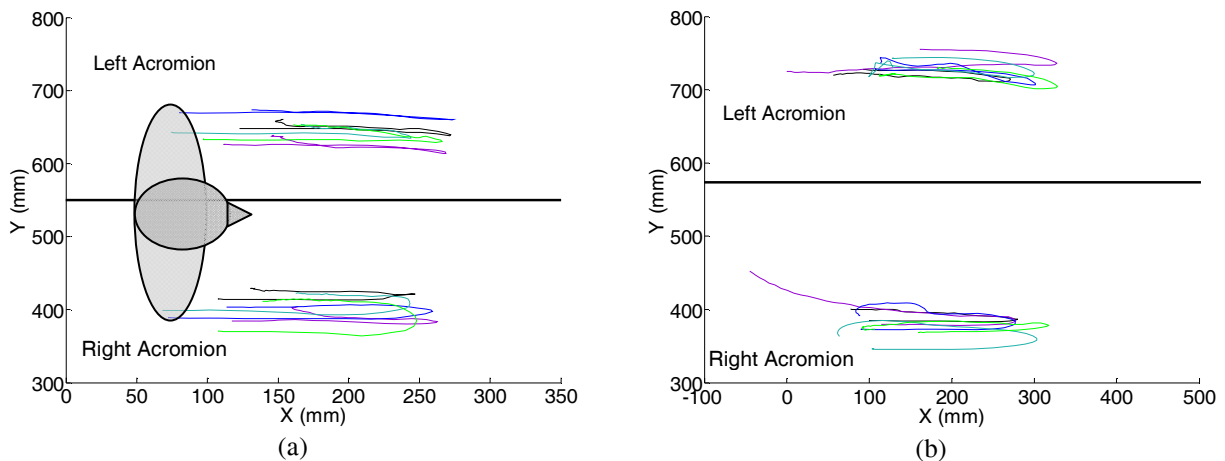


**Figure 11. Subject-Average left and right acromion marker trajectories in the transverse plane for the (a) child (superimposed by a schematic of a subject) and (b) adult group.**

## DISCUSSION AND CONCLUSIONS

This paper describes the development of method and device capable of providing a safe frontal pulse to restrained pediatric and adult human volunteers. While adult volunteers have previously been used in impact biomechanics, this effort represents the first to use child subjects in this manner. The envelope for a safe volunteer crash pulse was derived using a novel approach – determining the “pulse” associated with a bumper car to wall impact in an amusement park setting. From this envelope, a custom designed sled was constructed that allowed for the safe conduct of low speed frontal sled tests for the volunteers. Across the six trials for a single subject, the acceleration pulse is very repeatable. Both adult and child volunteers experience similar accelerations however the mass differences between the subject

groups lead to slightly greater restraint loading and rebound phases for the adults.

From the preliminary analyses of the head top marker trajectories, the adult subjects displayed a greater maximum displacement in the X-axis when compared to pediatric subjects. However, in the Z-axis, the pediatric group had a higher maximum displacement when compared to the adult group. This is indicative of a greater angular head rotation in children. Anatomic differences in the pediatric cervical spine – including more horizontal facets, ligaments with increased laxity, and a higher fulcrum of rotation – likely lead to these differences. It is important to note that these results demonstrate differences between adults and those 9-12 years – an age group which is not universally considered “pediatric” from a biomechanical perspective.

Future studies will combine data from the angular rate sensor with the head trajectories to understand the nature and timing of these differences in head rotation. Normalization schemes using anthropometric measures will shed insight into whether this variability is truly age dependent or can be explained by differences in size. .

Previous rear impact studies of adult human volunteers exposed to repeated acceleration of similar magnitude demonstrated a habituation response of the neck muscles, thereby leading to muscle relaxation with subsequent exposure (Blouin et al., 2003). In this study the pediatric and adult volunteers were subjected to a series of six frontal impacts of equal magnitude. If there is attenuation in neck muscle response with repeated exposure, one would expect increased head excursion in subsequent trials. But, no such trends were observed in these tests. Future work will correlate the dynamic EMG activity to the head and neck kinematics.

Several limitations of this approach need to be discussed. First, the head and neck trajectories were measured using a 'state of the art' 3D motion capture system utilizing markers affixed to the skin. Some error exists in assuming these skin markers exactly match the movement of the skeletal structures they represent. The magnitude of this error can be assessed by examining the time change of the distance between markers affixed to points on the same rigid body. For the head and neck, these differences are less than 2%. Second, examination of the acromion trajectories in the transverse plane revealed little movement perpendicular to this plane. Subjects primarily moved in the sagittal plane. For this reason, in this manuscript, although, three dimensional data were recorded, only two dimensional analyses were performed. The 2D plots of the marker trajectories were projections of the 3D trajectories on the sagittal plane. This approach may lead to slight under estimation of marker displacements.

In the absence of traditional efforts to define biomechanical response for children using pediatric PMHS, this approach represents a novel means by which to obtain important data that is needed for the design of biofidelic ATDs. By subjecting living child volunteers to sub-injurious dynamic loading, we gain a quantitative understanding of how real children move compared to adults. The human volunteer work described herein is part of a larger project in collaboration with University of Virginia and Takata Corporation in which adult PMHS will be subjected to crashes similar to those experienced by the

volunteers and then those same PMHS will be loaded at crash relevant speeds. The synthesis of the volunteer data with the adult PMHS data using either traditional scaling methods and/or computational models will greatly increase our knowledge of the biomechanics of child occupants, leading to better tools for optimizing protection of these occupants in motor vehicle crashes.

## ACKNOWLEDGEMENTS

The authors would like to thank all the human volunteers who participated in this study for their patience and willingness to take part in this research, Richard Kent, PhD (University of Virginia) for his assistance in design of the LASB and Ewout van der Laan, MSc (Technical University of Eindhoven, The Netherlands) for helping design the sled control system. The authors would like to acknowledge Takata Corporation, Japan for their collaboration and financial support for this study. The results presented in this report are the interpretation solely of the author(s) and are not necessarily the views of Takata Corporation.

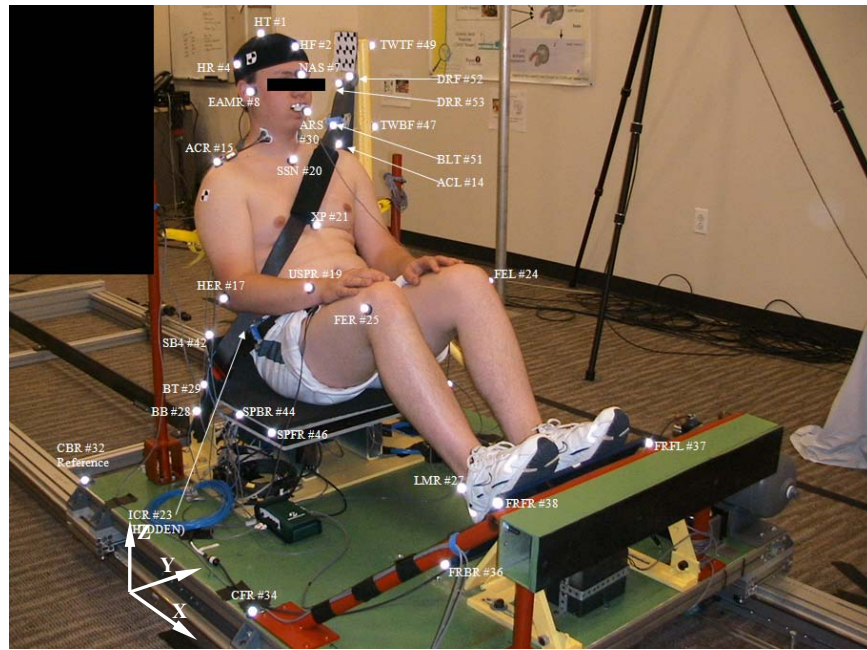
## REFERENCES

- Adekoya, N., D. Thurman, D. White and K. Webb (2002) "Surveillance for traumatic brain injury deaths – United States, 1989-1998." *MMWR Surveill Summ.* 51(10): 1-14.
- Arbogast K.B., J.S. Jermakian, Y. Ghali, R. Smith, R.A. Menon and M.R. Maltese (2005) "Patterns and predictors of pediatric head injury." *Proceedings of the International Research Conference on the Biomechanics of Impact, Prague, Czech Republic.*
- Arbogast, K. B., I. Chen, D. Durbin and F. K. Winston (2004). "Injury risks for children in child restraint systems in side impact crashes." *Proceedings of the International Research Conference on the Biomechanics of Impact, Graz, Austria.*
- Arbogast, K. B., R. A. Cornejo, M. J. Kallan, F. K. Winston and D. R. Durbin (2002) "Injuries to children in forward-facing child restraints." *Annu Proc Assoc Adv Automot Med* 46: 213-30.
- Blouin J.S., M. Descarreaux, A. Blanger-Gravel, M. Simoneau and N. Teasdale (2003) "Attenuation of human neck muscle activity following repeated imposed trunk-forward linear acceleration." *Experimental Brain Research.* 150:458-464
- Braksiek R.J and D. Roberts (2002) "Amusement Park Injuries and Deaths." *Annals of Emergency Medicine.* 39:1

- CDC growth charts (2000) Center for Disease Control and Prevention Growth Charts – Published May 30, 2000. <http://www.cdc.gov/GrowthCharts/>
- Durbin, D. R., M. R. Elliott and F. K. Winston (2003) “Belt-positioning booster seats and reduction in risk of injury among children in vehicle crashes.” *JAMA* 289(21): 2835-40.
- Ewing C.L., D.J. Thomas, G.W. Beeler, L.M. Patrick and D.B. Gillis (1968) “Dynamic response of head and neck of living human to gravity impact acceleration.” Proceedings of the twelfth Stapp Car Crash Conference. P-26. Paper 680792. Society of Automotive Engineers Inc.,
- Howard, A., L. Rothman, A. McKeag et al (2003) “Children in side impact motor vehicle crashes: seating positions and injury mechanisms.” *Journal of Trauma* 56: 1276-1285.
- Kallieris, D., G. Schmidt, J. Barz, R. Mattern and F. Schulz (1978) “Response and Vulnerability of the Human Body at Different Impact Velocities in Simulated Three-Point Belted Cadaver Tests.” *Proc. IRCOBI*, pp.105-209
- Malott, A., C. Parenteau, S. Marigowda and K. Arbogast (2004) “Sled test results using the Hybrid III 6 year olds: an evaluation of various restraints and crash configurations.” SAE World Congress, Detroit, MI, Society of Automotive Engineers.
- Menon, R., Y. S. Ghati, S. Ridella, S. Roberts and F. K. Winston (2003) “Evaluation of restraint type and performance tested with 3- and 6-year-old Hybrid III dummies at a range of speeds.” SAE 2003 World Congress.
- Mertz H.J and L.M. Patrick (1971) “Strength and response of the human neck.” Proceedings of the fifteenth Stapp Car Crash Conference. P-39. Paper 710855. Society of Automotive Engineers Inc.,
- NHANES data (1994) Center for Disease Control and Prevention Anthropometric reference data (1988 - 1994) [http://www.cdc.gov/nchs/about/major/nhanes/anthropometric\\_measures.htm](http://www.cdc.gov/nchs/about/major/nhanes/anthropometric_measures.htm)
- Orzechowski, K., E. Edgerton, D. Bulas et al (2003) “Patterns of injury to restrained children in side impact motor vehicle crashes: the side impact syndrome.” *Journal of Trauma* 54: 1094-1101.
- Reed M.P., S.M. Ebert-Hamilton and L.W. Schneider (2005) “Development of ATD Installation Procedures Based on Rear-Seat Occupant Postures.” Proceedings of the 49<sup>th</sup> Stapp Car Crash Conference. P-394. Paper 2005-22-0018. Society of Automotive Engineers Inc.,
- Shaw, C, R. Kent, E. Sieveka and J. Crandall (2001) “Spinal kinematics of restrained occupants in frontal impacts.” IRCOBI Conference on the Biomechanics of Impact, Isle of Man.
- Sherwood, C., C. Shaw, L. V. Rooij, R. Kent, J. Crandall, K. Orzechowski, M. Eichelberger and D. Kallieris (2003) “Prediction of cervical spine injury risk for the 6-year-old child in frontal crashes.” *Traffic Inj Prev* 4(3): 206-213.
- Stapp, J. (1949). “Human response to linear deceleration.” AF Technical Report 5915
- Thompson, M. and J. Irby (2003) “Recovery from mild head injury in pediatric populations.” *Seminars in Pediatric Neurology* 10(2): 130-139.
- Wismans, J., M. Phillippens, E. van Oorschot, D. Kallieris and R. Mattern (1987) “Comparison of human volunteer and cadaver head-neck response in frontal flexion.” Stapp Car Crash Conference.
- Zuckerbraun, BS, K. Morrison, B. Gaines, H.R. Ford, D.J. Hackam (2004) “Effect of Age on Cervical Spine Injuries in Children After Motor Vehicle Collisions: Effectiveness of Restraint Devices.” *J Pediatr Surg* 39:483-486.

**APPENDIX**

<b>Table A1.</b>					
<b>List of motion analysis marker locations on the subject and seating buck</b>					
<b>Marker #</b>	<b>Name</b>	<b>Abbreviation</b>	<b>Marker #</b>	<b>Name</b>	<b>Abbreviation</b>
1	Head Top	HT	28	Buckle Bottom	BB
2	Head Front	HF	29	Buckle Top	BT
3	Head Left	HL	30	Angular Rate Sensor	ARS
4	Head Right	HR	31	Cart Back-Left	CBL
5	Opisthocranium	OP	32	Cart Back-Right	CBR
6	EAM Left	EAML	33	Cart Front-Left	CFL
7	Nasion	NAS	34	Cart Front-Right <b>Reference</b>	CFR
8	EAM Right	EAMR	35	Foot Rest Back Left	FRBL
9	C4	C4	36	Foot Rest Back Right	FRBR
10	T1	T1	37	Foot Rest Front Left	FRFL
11	T4	T4	38	Foot Rest Front Right	FRFR
12	T8	T8	39	Seatback 1	SB1
13	T12	T12	40	Seatback 2	SB2
14	Acromion Left	ACL	41	Seatback 3	SB3
15	Acromion Right	ACR	42	Seatback 4	SB4
16	Humeral Epicondyle Left	HEL	43	Seatpan Back-Left	SPBL
17	Humeral Epicondyle Right	HER	44	Seatpan Back-Right	SPBR
18	Ulnar Styloid Process Left	USPL	45	Seatpan Front-Left	SPFL
19	Ulnar Styloid Process Right	USPR	46	Seatpan Front-Right	SPFR
20	Supra-Sternal Notch	SSN	47	Tower Bottom-Front	TWBF
21	Xiphoid Process	XP	48	Tower Bottom-Rear	TWBR
22	Iliac Crest Left	ICL	49	Tower Top-Front	TWTF
23	Iliac Crest Right	ICR	50	Tower Top-Rear	TWTR
24	Femoral Epicondyle Left	FEL	51	Belt	BLT
25	Femoral Epicondyle Right	FER	52	D-Ring Front	DRF
26	Lateral Malleolus Left	LML	53	D-Ring Rear	DRR
27	Lateral Malleolus Right	LMR			



(a)



(b)

**Figure A1.** (a) Frontal view and (b) rear view of an adult subject seated in LASB with all motion analysis markers labeled. The local coordinate axes along with the reference marker is shown.